

# High time resolution ambient observations of gas-phase perfluoroalkyl carboxylic acids: Implications for atmospheric sources

## Authors

Cora J. Young,<sup>1\*</sup> Shira Joudan,<sup>1,2</sup> Ye Tao,<sup>1,3</sup> Jeremy J.B. Wentzell,<sup>4</sup> John Liggio<sup>4\*</sup>

<sup>1</sup> Department of Chemistry, York University, Toronto, Canada

<sup>2</sup> Department of Chemistry, University of Alberta, Edmonton, Canada

<sup>3</sup> Department of Chemistry, University of Toronto, Toronto, Canada

<sup>4</sup> Air Quality Research Division, Environment and Climate Change Canada, Toronto, Canada

\*Correspondence to [youngcej@yorku.ca](mailto:youngcej@yorku.ca), [john.liggio@ec.gc.ca](mailto:john.liggio@ec.gc.ca)

## Abstract

Atmospheric formation of persistent perfluoroalkyl carboxylic acids (PFCAs) is a route to global contamination, including drinking water sources. We present high time resolution measurements of C<sub>2</sub>-C<sub>6</sub> PFCAs in ambient air made over 6 weeks each in winter and summer 2022 in Toronto, Canada. Observations were made using chemical ionization mass spectrometry with acetate ionization with care taken to avoid system contamination. Measurements of trifluoroacetic acid (C<sub>2</sub> PFCA) are reported at 1-minute time resolution, while those for C<sub>3</sub>-C<sub>6</sub> PFCAs are at 10-minute time resolution. Variations with time and relationships to meteorology and other pollutants show evidence of secondary formation of all observed PFCAs except perfluoropropionic acid (C<sub>3</sub> PFCA). High time resolution data allows these unique observations, allowing for improved process and source understanding moving forward. Mixing ratios of TFA

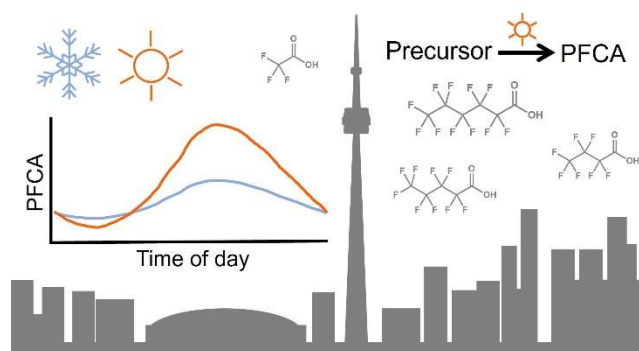
were higher than predicted from models that describe TFA formation from known precursors indicating additional atmospheric sources of this molecule have yet to be identified.

## Keywords

Perfluoroalkyl carboxylic acid (PFCA), PFAS, trifluoroacetic acid (TFA), atmospheric monitoring, atmospheric formation, source attribution, acetate chemical ionization mass spectrometry (CIMS)

**Synopsis** High time resolution measurements of gaseous perfluoroalkyl carboxylic acids using acetate chemical ionization mass spectrometry allowing insight into their sources

## TOC art



## Introduction

Perfluoroalkyl carboxylic acids (PFCAs,  $F(CF_2)_nCOOH$ ) are a class of persistent compounds that are found globally, among which several are bioaccumulative and toxic.<sup>1–3</sup> PFCAs are one of the most problematic sub-classes of per- and polyfluoroalkyl substances (PFAS). Multiple jurisdictions have proposed class-based regulations for PFAS to counter their negative impacts.<sup>4,5</sup> Regulations are currently in place for PFCAs and their precursors with  $\geq 8$  carbons, leading to replacements based on short-chain ( $\leq 7$  carbons) and ultra-short-chain ( $\leq 4$  carbons) C-F backbones.<sup>6,7</sup> Thus, observed short- and ultra-short-chain PFCA levels in the

environment have been increasing.<sup>8</sup> Recent studies have shown particularly large increases in the environmental abundance of C<sub>2</sub> PFCA, trifluoroacetic acid (TFA).<sup>9,10</sup>

Short-chain PFCAs are volatile in their acidic form and can be emitted to air from point sources (e.g., industrial facilities,<sup>11</sup> fluoropolymer thermolysis,<sup>12</sup> wastewater treatment plants<sup>13,14</sup>), though as strong acids they are expected to have short atmospheric lifetimes.<sup>15</sup> Their presence in remote terrestrial regions can be attributed primarily to atmospheric oxidation from volatile PFAS, such as fluorotelomer compounds, hydrochlorofluorocarbons (HCFCs), and hydrofluorocarbons (HFCs), with shorter-chain PFCAs having more precursors.<sup>10,16,17</sup> Atmospheric formation impacts atmospheric PFCA levels globally,<sup>15,18–20</sup> though the relative importance of direct emission, remobilization of PFCAs (e.g., by sea spray aerosols<sup>21</sup>), and atmospheric formation are not well understood. In samples derived from the atmosphere, PFCA abundance is generally inversely proportional to carbon chain length, with TFA levels much higher than all others.<sup>18,22</sup>

Understanding the sources and fate of atmospheric PFCAs has been hampered by analytical methods. Measurements of atmospheric PFCAs have been made using time-integrated samples, such as atmospheric deposition or air collected onto sorbents/denuders, followed by offline analysis (e.g.,<sup>13,14,18,19,23</sup>). This limits the temporal resolution of the samples to several days to months, though a single study measured TFA using denuders over five days with a time resolution of four hours.<sup>24</sup> Atmospheric conditions can change quickly, with parameters that affect chemistry (e.g., solar irradiance) changing on the timescales of minutes to hours. Fast, in-situ measurements that can determine atmospheric concentrations on similar timescales to these atmospheric processes are needed to improve our understanding of PFCA chemistry and sources. A method commonly used to measure atmospheric acids at high time resolution is chemical

ionization mass spectrometry (CIMS, e.g.,<sup>25–28</sup>). Detection of PFCAs using CIMS has been demonstrated in the lab with iodide<sup>29,30</sup> and acetate<sup>31</sup> ionizations. Recently, TFA was observed in ambient air using iodide-CIMS, though <1% of measurements were above the limit of detection.<sup>32</sup>

Here, we quantify ambient gaseous PFCAs using CIMS in an urban region across two seasons. This first application of CIMS to quantify ambient PFCAs will be used to assess the importance of high time resolution data to understand their sources.

## Methods

The CIMS was a modified version of that used previously.<sup>33</sup> Modifications included altering the method of pressure control and reagent ion delivery, as well as replacing the stainless-steel ion molecule reactor with a polytetrafluoroethylene custom design (Figure S1) that was operated at lower pressures than previously described. The time resolution of the instrument was 10 s. Prior to use, all fluoropolymer components were pre-cleaned by sonicating in deionized water and baking at 80 °C in a vacuum oven (<0.5 mBar) for 24 hours.

Calibration was performed using acetate ionization with a Fluigent microfluidic control system to generate microlitre flows of aqueous acids into a nebulizer housed in a heated oven. Rapid and quantitative evaporation resulted in gaseous acids from the liquid solutions, which were diluted and added at various concentrations via a pre-cleaned perfluoroalkoxy alkane inlet to the CIMS. The calibration source output for TFA was validated by denuder collection and offline analysis,<sup>34,35</sup> but not for other PFCAs. The ratio of measured versus calculated output from the aqueous concentration for TFA was applied to the other PFCAs (see SI Text S1, Table S1).

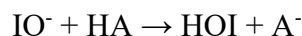
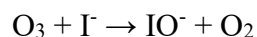
Measurements were made in Toronto, Canada at two locations (separated by ~4 km) during 2021 and 2022 (Figure S2). In 2021, measurements were made at the York University rooftop (43.7738 N, 79.5071 W) from 29 August to 6 September using iodide ionization. In 2022, measurements were made at Environment and Climate Change Canada (ECCC) Downsview (43.7814 N, 79.4685 W) from 8 February to 10 April ('winter') and 26 June to 22 August ('summer') using acetate ionization. All times are in Eastern Standard Time (EST, UTC – 5). Samples were collected through a polyethylene inlet (1/4" outer diameter; 3/16" inner diameter; length ~2 m in 2021, 1.5 m in 2022). Automated blanks were conducted for 10 min every hour by overflowing the inlet near the sampling end with air passed through a 400 °C Pt catalyst and acid trapping filter material (sodium bicarbonate; United filtration Inc.). These blanks accounted for potential off-gassing from inlet and CIMS components. The ECCC location was co-located with a National Air Pollution Surveillance Program site that measures several pollutants (e.g., O<sub>3</sub>, CO). Irradiance measurements were made at the York University site. Limits of detection (LODs) for PFCAs were calculated according to Bertram et al.<sup>36</sup> Three times the standard deviation of each blank signal was used to create real-time LODs. Ambient signals were compared to the LOD determined from the blank collected immediately before. The decrease in signal at the onset of the blanks was also used to assess the instrument response time for TFA. Analyte signals were normalized to reagent ion signals and background subtracted. Further details regarding instrument configuration, calibrations, and ambient measurements can be found in the supporting information.

## Results and Discussion

### *Method performance: I-CIMS, and acetate CIMS*

Fluoropolymers are a known source of PFCAs<sup>25,35</sup> with previous CIMS instruments noting PFCA ions in their background measurements, which were attributed to fluoropolymers in the instrument and inlet.<sup>25</sup> Our instrument modifications resulted in background signals that were relatively clean of PFCA signals (Figure S3) although non-zero, resulting in LODs that made ambient measurements at the expected low levels achievable.

Measurements in summer 2021 using I-CIMS resulted in signals attributable to PFCAs, with TFA as the highest signal. We observed masses consistent with the TFA iodide adduct ( $m/z$  240.897,  $C_2F_3O_2HI^-$ ) and the conjugate base of TFA ( $m/z$  112.985,  $C_2F_3O_2^-$ ). The iodide adduct signal was always larger (by >3.65 times) and relative signals were highly variable (Figure S4). Previous I-CIMS PFCA laboratory measurements reported adducts as the dominant ions with small quantities of the conjugate bases, which were attributed to proton transfer to the reagent ion (see SI).<sup>30</sup> However, the variability of our relative ion signals suggests that ambient measurement conditions were affecting the ionization. An ozone-dependent competing ionization mechanism for I-CIMS has been previously reported for acids.<sup>37,38</sup> Iodine oxides (e.g.,  $IO^-$ ) formed from reaction between the iodide reagent ion and ambient ozone could react with acids (HA) to form their conjugate base via proton transfer:



We observed higher ratios of conjugate base to adduct at higher levels of ambient ozone, during which higher  $IO^-$  was also observed (Figure S4). This is qualitatively consistent with the proposed ozone-dependent ionization.<sup>37,38</sup> Thus, quantification of ambient PFCAs using I-CIMS

would be complex, likely requiring multi-dimensional calibrations involving humidity and ozone corrections. To avoid interferences and simplify CIMS application to PFCAs, I-CIMS was not pursued further, and an alternate ionization (acetate) applied.<sup>31</sup>

Measurements in 2022 in winter and summer using acetate-CIMS resulted in signals attributable to several PFCAs. All PFCAs were observed solely as their conjugate base ion without any ozone or humidity dependencies.<sup>31</sup> In winter, all PFCAs from TFA (C<sub>2</sub>) to PFHxA (C<sub>6</sub>) were detectable. In summer, PFPrA (C<sub>3</sub>) could not be measured because of another insufficiently resolved peak in the mass spectrum.

The acetate-CIMS response time for TFA was determined by fitting a double exponential function to the signal decrease upon the onset of each blank. Median response times, defined as the e-folding time (1/e) were faster than 25 s, with the slowest response times remaining less than 1 min (Figure S5). Thus, 1-min TFA measurements can be reliably reported for this configuration. The 1-min LODs for TFA ranged from 0.010 to 0.407 pptv ( $10^{-12}$  mol mol<sup>-1</sup>), which are comparable to the lowest LODs reported for CIMS measurements for any chemical using any ionization (Tables S2, S3, Figure S6).<sup>32,36,39,40</sup> Among over 145,000 1-min TFA measurements, 92.63 % were above LOD. All other PFCAs had lower observed signals, so data was averaged to 10 min. For these compounds, LODs were <46 ppqv ( $10^{-15}$  mol mol<sup>-1</sup>, Table S2) and detection frequencies ranged from 92 % for PFBA to >99 % for PFPeA and PFHxA (Table S4).

#### *Ambient measurements of gaseous TFA*

Observed mixing ratios of TFA ranged from <LOD to 1.72 pptv (<LOD to ~8.76 ng m<sup>-3</sup>; Figure 1, Table S1, estimated mass concentrations in SI). Our measurements are generally consistent with previous gas-phase TFA measurements made with denuders in the United States,

Canada, and China between 1994 and 2021<sup>23,24,34,41,42</sup> and with I-CIMS in the United States in 2023<sup>32</sup> (Table S6). Seven 48-hr gaseous TFA measurements were made in Toronto between June and December 2000, reporting a median of 0.25 pptv (range 0.06 to 1.06 pptv).<sup>23</sup> We can compare directly to these observations using a moving 48-hr average of our measurements, which leads to winter and summer median values of 0.40 and 0.51 pptv, respectively (range of 0.24 to 0.84 pptv, Figure S6). Thus, our mean measurements are about two times higher than, but within the range of, the measurements made in 2000. This is surprising, given that TFA has been shown to be rapidly increasing in the atmosphere over this period.<sup>9,10</sup> We note that some previous TFA measurements, including those made in Toronto, used PFPrA acid as an internal standard,<sup>24,42</sup> for which the presence of atmospheric PFPrA<sup>10,18</sup> could have affected the accuracy.

Mixing ratios for TFA were generally higher in summer, with a median of 0.412 pptv (<LOD to 0.932 pptv) in winter and 0.519 pptv (<LOD to 1.511 pptv) in summer (Figure 1, Table 1). Similar seasonal differences have previously been observed in samples collected over one year in Canada,<sup>23</sup> and over several years in Beijing.<sup>24,42,43</sup> We also observed that mixing ratios were generally higher during the day (Figures 1, 2). The highest average TFA was observed at 15:00 EST in winter and 16:30 in summer and the lowest at 06:30 in winter and 05:30 in summer. This is consistent with a previous study that measured gaseous TFA with 4-hr time resolution over five days in January in Beijing.<sup>24</sup>



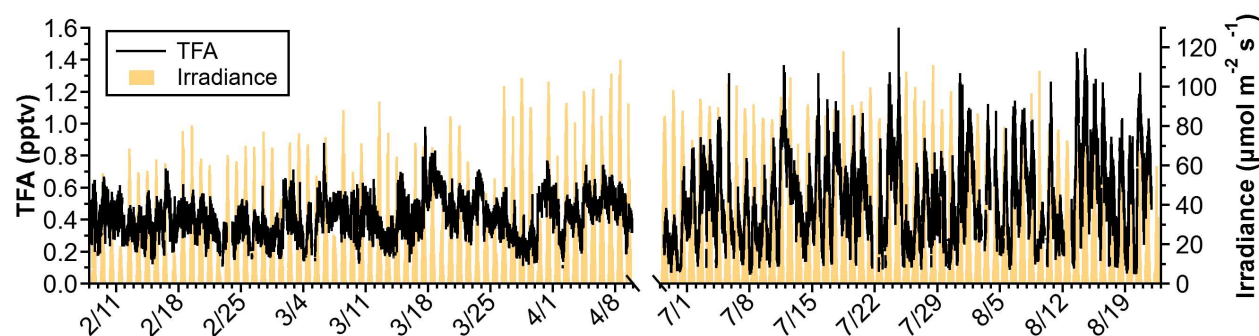


**Figure 1.** Ambient measurements of TFA from 2022 in Toronto, Canada using acetate-CIMS.

Mixing ratios at a timescale of 1 min (black line, left axis) are shown along with measured irradiance (orange shading, right axis).

#### *Ambient measurements of other gaseous PFCAs*

In the absence of calibration correction factors for C<sub>3</sub> to C<sub>6</sub> PFCAs, we estimated their mixing ratios using information from TFA corrections. While mixing ratios estimated with this approach are more uncertain (estimated  $\pm 150\%$ , Table S1), relative variations are reliable. To our knowledge, gaseous PFCAs  $\geq C_4$  have been measured at timescales  $\geq 2$  days,<sup>22</sup> while the rare measurements of gaseous PFPrA have been made by sampling for  $>1$  month.<sup>34,44</sup> We observed median levels in the range of 10s of ppqv for PFCAs in both seasons, with levels higher in summer than winter (Table S5). Generally, PFPrA was highest and PFBA was lowest. This contrasts the few existing atmospheric samples, in which levels decreased with increasing chain length (e.g.,<sup>10,18,34</sup>). Given the uncertainties in our estimated mixing ratios and the known issues associated with offline gaseous PFCA sampling,<sup>45,46</sup> it is challenging to quantitatively compare our results to previous reports. For C<sub>4</sub>-C<sub>6</sub> PFCAs, a diurnal variation was observed in both winter and summer, though a much stronger variation was seen in summer (Figure 2B). For PFPrA,

there was no discernible variation in signal with time of day. These represent the first observations of time-of-day variation for  $\geq C_3$  PFCAs.

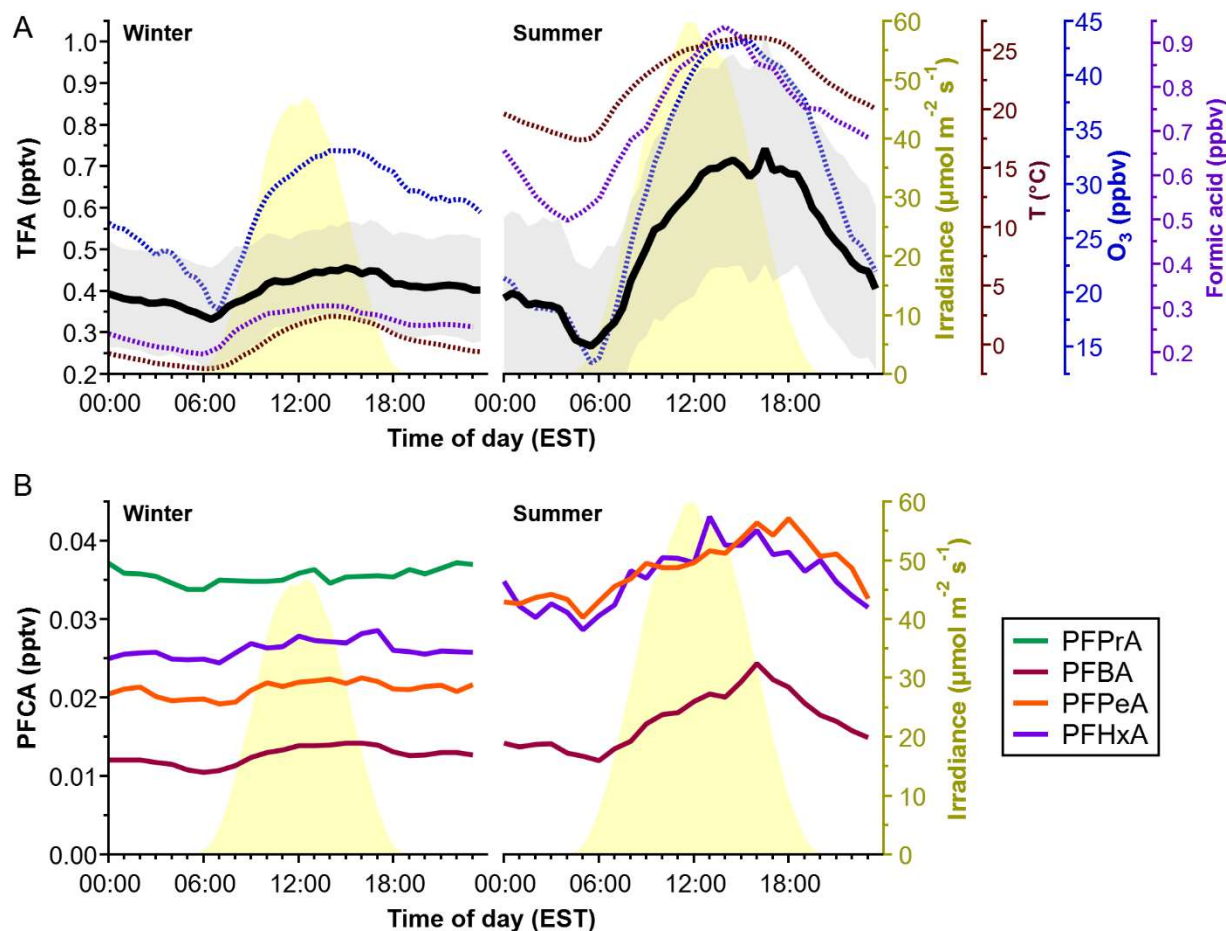


**Figure 2.** Winter (left) and summer (right) for A) average measured TFA (black line shown with standard deviation in grey shading), formic acid (purple), O<sub>3</sub> (blue), temperature (red), and irradiance (yellow) to 30 min timescale, and B) average estimated C<sub>3</sub>-C<sub>6</sub> PFCAs (PFPrA, PFBA, PFPeA, PFHxA, coloured lines) with mean irradiance (yellow shading) diurnally averaged to one hour timescale. For clarity, standard deviations are omitted for everything except TFA.

## 201 *Gaseous PFCA source attribution*

202 High time response measurements allow us to better understand PFCA sources by  
203 relating changes in concentrations to other quickly changing variables (e.g., wind direction),  
204 which is impossible with time integrated samples. Higher levels during the day were observed  
205 for PFCAs except PFPrA (Figures 2B, S6, S7). Both irradiance and temperature are higher  
206 during daytime, indicating that increased gaseous PFCAs could result from atmospheric  
207 formation or gas-particle partitioning. For PFPrA, we observed positive correlations with formic  
208 acid ( $r=0.56$ ) and temperature ( $r=0.59$ ). For all other PFCAs, positive correlations with ozone  
209 ( $0.29 < r < 0.59$ ), formic acid ( $0.39 < r < 0.50$ ), and temperature ( $0.31 < r < 0.52$ ) were seen (Figure S8).  
210 These correlations represent the strongest among all environmental variables tested. Correlations  
211 with photochemically-formed ozone and formic acid suggest that atmospheric formation is an  
212 important source of PFCAs in Toronto. Correlations with temperature are consistent with  
213 atmospheric formation but could suggest the role of gas-particle partitioning. However, most of  
214 these PFCAs are expected to reside in the gas phase<sup>23,24,42–44,46</sup> and correlations between PFCAs  
215 and PM<sub>2.5</sub> were negligible ( $r < 0.1$ ) and independent of humidity (Figure S9). This suggests gas-  
216 particle partitioning may act as a minor PFCA source. It is also possible that point sources<sup>11–14,47</sup>  
217 could directly release gaseous PFCAs. Similar PFCA levels were measured from all wind  
218 directions, with slightly higher levels associated with southwest winds (Figures S10, S11).  
219 Airmasses arriving in Toronto from the southwest are known to be more polluted and enrichment  
220 with southwest winds is common for other pollutants.<sup>48,49</sup> Weak to negligible correlations were  
221 observed between PFCAs and chemical markers for direct emissions, such as CO ( $-0.13 < r < 0.14$ )  
222 and SO<sub>2</sub> ( $r < 0.16$ , Figure S8), suggesting a minimal contribution of direct emissions. Some  
223 pollutant sources may also differ between weekdays and weekends/holidays.<sup>50</sup> For PFCAs except

PFPrA, levels were generally higher on weekends, with some time periods significantly higher (Table S7). This is consistent with lower weekend  $\text{NO}_x$  ( $\equiv \text{NO} + \text{NO}_2$ ), where yields of atmospherically-formed PFCAs (and ozone<sup>50</sup>) are higher under lower  $\text{NO}_x$  conditions.<sup>15,51,52</sup> Overall, our observations most strongly support atmospheric formation as the major source of PFCAs, with a potential small contribution of gas-particle partitioning.

For TFA atmospheric formation, several modelling studies have examined the potential for volatile organofluorine compounds to contribute to gaseous TFA. Models generally predict 10s of ppqv of TFA or its immediate precursors (i.e., trifluoroacetyl halides) from degradation of HCFCs and HFCs for the region including Toronto,<sup>53–55</sup> which is much lower than our observations, indicating the importance of other sources. Recently introduced hydrofluoroolefins (HFOs) that produce TFA in high yields represent an additional potential source. For example, predicted Toronto mixing ratios for full-scale implementation of HFO-1234yf into mobile air conditioners are up to 1 pptv.<sup>20,55</sup> These models are in reasonable agreement with our observations, though they represent usage scenarios where all vehicles contain HFO-1234yf, which is not currently the case. Thus, we suggest there are additional precursor sources that contribute to gaseous TFA. Numerous additional TFA precursors are known to be present in the atmosphere (e.g., halogenated anaesthetics, fluorotelomer compounds)<sup>51</sup> for which predicted atmospheric levels do not exist. Given that our observations of TFA are consistent with atmospheric formation as the dominant source, further work is needed to identify specific TFA precursor molecules as well as better constrain the sources of longer-chain PFCAs for which no model-predicted gaseous levels exist.

## Implications

We quantified gas-phase TFA with 1-min time resolution and C<sub>3</sub>-C<sub>6</sub> PFCAs with 10-min time resolution in Toronto, with the strongest evidence indicating photochemical production as the dominant source for all PFCAs except PFPrA. This indicates atmospheric formation is an important source of PFCAs in urban areas as well as remote regions. Our observations underscore the need for further atmospheric measurements of both PFCAs and their potential precursors. While predictions<sup>46</sup> and limited reliable measurements<sup>23,24,42-44</sup> suggest these PFCAs are predominantly in the gas phase, the overall importance of particulate phase PFCAs as a source and/or sink of gaseous PFCAs is not well understood. Lastly, the abundance of PFCAs in air also demonstrates the importance of understanding inhalation as an exposure pathway, which is currently unknown.

## ASSOCIATED CONTENT

**Supporting Information.** Detailed descriptions and additional information on instrumentation, calibrations, QA/QC, and atmospheric observations. There are references not cited in the main text.<sup>56,57</sup>

## Acknowledgements

We thank Jessica Clouthier, Eric Vanhauwaert, Mayré Rodríguez, Andrea Angelucci, and Trevor VandenBoer. Thanks to Ontario Ministry of the Environment, Conservation and Parks for maintenance of the Toronto North station. Funding was provided by the Natural Science and Engineering Research Council and the Chemicals Management Plan of the Government of Canada.

## References

- (1) Martin, J. W.; Mabury, S. A.; Solomon, K. R.; Muir, D. C. G. Bioconcentration and Tissue Distribution of Perfluorinated Acids in Rainbow Trout (*Oncorhynchus Mykiss*). *Environ Toxicol Chem* **2003**, 22 (1), 196–204.
- (2) Secretariat of the Stockholm Convention. *Stockholm Convention on Persistent Organic Pollutants (POPs) as Amended in 2009, 2011, 2013, and 2015*; 2015. [chm.pops.int](http://chm.pops.int).
- (3) Fenton, S. E.; Ducatman, A.; Boobis, A.; DeWitt, J. C.; Lau, C.; Ng, C.; Smith, J. S.; Roberts, S. M. Per- and Polyfluoroalkyl Substance Toxicity and Human Health Review: Current State of Knowledge and Strategies for Informing Future Research. *Environ Toxicol Chem* **2021**, 40 (3), 606–630. <https://doi.org/10.1002/etc.4890>.
- (4) OECD. *Toward a New Comprehensive Global Emission Inventory of Per- and Polyfluoroalkyl Substances (PFASs) - Summary Report on Updating the OECD 2007 List of per- and Polyfluoroalkyl Substances (PFASs)*; Paris, 2018.
- (5) Bălan, S. A.; Mathrani, V. C.; Guo, D. F.; Algazi, A. M. Regulating PFAS as a Chemical Class under the California Safer Consumer Products Program. *Environ Health Perspect* **2021**, 129 (2), 1–9. <https://doi.org/10.1289/EHP7431>.
- (6) Wang, Z.; Cousins, I. T.; Scheringer, M.; Hungerbuehler, K. Hazard Assessment of Fluorinated Alternatives to Long-Chain Perfluoroalkyl Acids (PFAAs) and Their Precursors: Status Quo, Ongoing Challenges and Possible Solutions. *Environ Int* **2015**, 75, 172–179. <https://doi.org/10.1016/j.envint.2014.11.013>.
- (7) Glüge, J.; Scheringer, M.; Cousins, I. T.; DeWitt, J. C.; Goldenman, G.; Herzke, D.; Lohmann, R.; Ng, C. A.; Trier, X.; Wang, Z. An Overview of the Uses of Per- and Polyfluoroalkyl Substances (PFAS). *Environ Sci Process Impacts* **2020**, 22 (12), 2345–2373. <https://doi.org/10.1039/D0EM00291G>.
- (8) Gewurtz, S. B.; Auyeung, A. S.; De Silva, A. O.; Teslic, S.; Smyth, S. A. Per- and Polyfluoroalkyl Substances (PFAS) in Canadian Municipal Wastewater and Biosolids:

Recent Patterns and Time Trends 2009 to 2021. *Science of The Total Environment* **2024**, 912, 168638. <https://doi.org/10.1016/j.scitotenv.2023.168638>.

(9) Freeling, F.; Scheurer, M.; Koschorreck, J.; Hoffmann, G.; Ternes, T. A.; Nödler, K. Levels and Temporal Trends of Trifluoroacetate (TFA) in Archived Plants: Evidence for Increasing Emissions of Gaseous TFA Precursors over the Last Decades. *Environ Sci Technol Lett* **2022**. <https://doi.org/10.1021/acs.estlett.2c00164>.

(10) Pickard, H. M.; Criscitiello, A. S.; Persaud, D.; Spencer, C.; Muir, D. C. G.; Lehnher, I.; Sharp, M. J.; De Silva, A. O.; Young, C. J. Ice Core Record of Persistent Short-Chain Fluorinated Alkyl Acids: Evidence of the Impact from Global Environmental Regulations. *Geophys Res Lett* **2020**, 47 (10). <https://doi.org/10.1029/2020GL087535>.

(11) Wang, P.; Zhang, M.; Li, Q.; Lu, Y. Atmospheric Diffusion of Perfluoroalkyl Acids Emitted from Fluorochemical Industry and Its Associated Health Risks. *Environ Int* **2021**, 146. <https://doi.org/10.1016/j.envint.2020.106247>.

(12) Ellis, D. A.; Mabury, S. A.; Martin, J. W.; Muir, D. C. G. Thermolysis of Fluoropolymers as a Potential Source of Halogenated Organic Acids in the Environment. *Nature* **2001**, 412, 321–324. <https://doi.org/10.1038/35085548>.

(13) Vierke, L.; Ahrens, L.; Shoeib, M.; Reiner, E. J.; Guo, R.; Palm, W. U.; Ebinghaus, R.; Harner, T. Air Concentrations and Particle-Gas Partitioning of Polyfluoroalkyl Compounds at a Wastewater Treatment Plant. *Environmental Chemistry* **2011**, 8 (4), 363–371. <https://doi.org/10.1071/EN10133>.

(14) Ahrens, L.; Shoeib, M.; Harner, T.; Lee, S. C.; Guo, R.; Reiner, E. J. Wastewater Treatment Plant and Landfills as Sources of Polyfluoroalkyl Compounds to the Atmosphere. *Environ Sci Technol* **2011**, 45 (19), 8098–8105. <https://doi.org/10.1021/es1036173>.



- 318 (15) Thackray, C. P.; Selin, N. E.; Young, C. J. Global Atmospheric Chemistry Model for the  
319 Fate and Transport of PFCAs and Their Precursors. *Environ Sci Process Impacts* **2020**,  
320 22, 285–293. <https://doi.org/10.1039/c9em00326f>.
- 321 (16) Garnett, J.; Halsall, C.; Winton, H.; Joerss, H.; Mulvaney, R.; Ebinghaus, R.; Frey, M.;  
322 Jones, A.; Leeson, A.; Wynn, P. Increasing Accumulation of Perfluorocarboxylate  
323 Contaminants Revealed in an Antarctic Firn Core (1958–2017). *Environ Sci Technol*  
324 **2022**, 56 (16), 11246–11255. <https://doi.org/10.1021/acs.est.2c02592>.
- 325 (17) Pickard, H.; Criscitiello, A.; Spencer, C.; Sharp, M. J.; Muir, D. C. G.; De Silva, A. O.;  
326 Young, C. J. Continuous Non-Marine Inputs of per- and Polyfluoroalkyl Substances to the  
327 High Arctic: A Multi-Decadal Depositional Record. *Atmos Chem Phys* **2018**, 18 (7), 5045–  
328 5058. <https://doi.org/10.5194/acp-2017-1009>.
- 329 (18) Scott, B. F.; Spencer, C.; Mabury, S. A.; Muir, D. C. G. Poly and Perfluorinated  
330 Carboxylates in North American Precipitation. *Environ Sci Technol* **2006**, 40 (23), 7167–  
331 7174.
- 332 (19) Pike, K. A.; Edmiston, P. L.; Morrison, J. J.; Faust, J. A. Correlation Analysis of  
333 Perfluoroalkyl Substances in Regional U.S. Precipitation Events. *Water Res* **2021**, 190,  
334 116685. <https://doi.org/10.1016/j.watres.2020.116685>.
- 335 (20) Wang, Z.; Wang, Y.; Li, J.; Henne, S.; Zhang, B.; Hu, J.; Zhang, J. Impacts of the  
336 Degradation of 2,3,3,3-Tetrafluoropropene into Trifluoroacetic Acid from Its Application in  
337 Automobile Air Conditioners in China, the United States and Europe. *Environ Sci Technol*  
338 **2018**, 52 (5), 2819–2826. <https://doi.org/10.1021/acs.est.7b05960>.
- 339 (21) Sha, B.; Johansson, J. H.; Salter, M. E.; Blichner, S. M.; Cousins, I. T. Constraining  
340 Global Transport of Perfluoroalkyl Acids on Sea Spray Aerosol Using Field  
341 Measurements. *Sci Adv* **2024**, 10 (14). <https://doi.org/10.1126/sciadv.adl1026>.



- 342 (22) Wu, J.; Jin, H.; Li, L.; Zhai, Z.; Martin, J. W.; Hu, J.; Peng, L.; Wu, P. Atmospheric  
343 Perfluoroalkyl Acid Occurrence and Isomer Profiles in Beijing, China. *Environmental*  
344 *Pollution* **2019**, 255. <https://doi.org/10.1016/j.envpol.2019.113129>.
- 345 (23) Martin, J. W.; Mabury, S. a; Wong, C. S.; Noventa, F.; Solomon, K. R.; Alaee, M.; Muir, D.  
346 C. G. Airborne Haloacetic Acids. *Environ Sci Technol* **2003**, 37 (13), 2889–2897.  
347 <https://doi.org/10.1021/es026345u>.
- 348 (24) Wu, J.; Martin, J. W.; Zhai, Z.; Lu, K.; Li, L.; Fang, X.; Jin, H.; Hu, J.; Zhang, J. Airborne  
349 Trifluoroacetic Acid and Its Fraction from the Degradation of HFC-134a in Beijing, China.  
350 *Environ Sci Technol* **2014**, 48 (2), 3675–3681. <https://doi.org/10.1021/es4050264>.
- 351 (25) Brophy, P.; Farmer, D. K. A Switchable Reagent Ion High Resolution Time-of-Flight  
352 Chemical Ionization Mass Spectrometer for Real-Time Measurement of Gas Phase  
353 Oxidized Species : Characterization from the 2013 Southern Oxidant and Aerosol Study.  
354 *Atmos Meas Tech* **2015**, 8 (7), 2945–2959. <https://doi.org/10.5194/amt-8-2945-2015>.
- 355 (26) Veres, P. R.; Roberts, J. M.; Cochran, A. K.; Gilman, J. B.; Kuster, W. C.; Holloway, J. S.;  
356 Graus, M.; Flynn, J.; Lefer, B.; Warneke, C.; de Gouw, J. Evidence of Rapid Production of  
357 Organic Acids in an Urban Air Mass. *Geophys Res Lett* **2011**, 38, L17807, doi:  
358 10.1029/2011GL048420.
- 359 (27) Roberts, J. M.; Veres, P.; Warneke, C.; Neuman, J. A.; Washenfelter, R. A.; Brown, S.  
360 S.; Baasandorj, M.; Burkholder, J. B.; Burling, I. R.; Johnson, T. J.; Yokelson, R. J.; de  
361 Gouw, J. Measurement of HONO, HNCO, and Other Inorganic Acids by Negative-Ion  
362 Proton-Transfer Chemical-Ionization Mass Spectrometry (NI-PT-CIMS): Application to  
363 Biomass Burning Emissions. *Atmos Meas Tech* **2010**, 3 (4), 981–990.  
364 <https://doi.org/10.5194/amt-3-981-2010>.
- 365 (28) Lutz, A.; Mohr, C.; Le Breton, M.; Lopez-Hilfiker, F. D.; Priestley, M.; Thornton, J. A.;  
366 Hallquist, M. Gas to Particle Partitioning of Organic Acids in the Boreal Atmosphere. *ACS*

367 *Earth Space Chem* **2019**, 3 (7), 1279–1287.  
 368 <https://doi.org/10.1021/acsearthspacechem.9b00041>.

369 (29) Riedel, T. P.; Lang, J. R.; Strynar, M. J.; Lindstrom, A. B.; Offenberg, J. H. Gas-Phase  
 370 Detection of Fluorotelomer Alcohols and Other Oxygenated per- and Poly Fluoroalkyl  
 371 Substances by Chemical Ionization Mass Spectrometry. *Environ Sci Technol Lett* **2019**, 6  
 372 (5), 289–293. <https://doi.org/10.1021/acs.estlett.9b00196>.

373 (30) Bowers, B. B.; Thornton, J. A.; Sullivan, R. C. Evaluation of Iodide Chemical Ionization  
 374 Mass Spectrometry for Gas and Aerosol-Phase per- and Polyfluoroalkyl Substances  
 375 (PFAS) Analysis. *Environ Sci Process Impacts* **2022**, 25 (2), 277–287.  
 376 <https://doi.org/10.1039/d2em00275b>.

377 (31) Veres, P. R.; Roberts, J. M.; Warneke, C.; Welsh-Bon, D.; Zahniser, M.; Herndon, S.;  
 378 Fall, R.; de Gouw, J. Development of Negative-Ion Proton-Transfer Chemical-Ionization  
 379 Mass Spectrometry (NI-PT-CIMS) for the Measurement of Gas-Phase Organic Acids in  
 380 the Atmosphere. *Int J Mass Spectrom* **2008**, 274, 48–55.  
 381 <https://doi.org/10.1016/j.ijms.2008.04.032>.

382 (32) Mattila, J. M.; Offenberg, J. H. Measuring Short-Chain per- and Polyfluoroalkyl  
 383 Substances in Central New Jersey Air Using Chemical Ionization Mass Spectrometry. *J*  
 384 *Air Waste Manage Assoc* **2024**, 74 (8), 531–539.  
 385 <https://doi.org/10.1080/10962247.2024.2366491>.

386 (33) Hayden, K. L.; Li, S.-M.; Liggio, J.; Wheeler, M. J.; Wentzell, J. J. B.; Leithead, A.;  
 387 Brickell, P.; Mittermeier, R. L.; Oldham, Z.; Mihele, C. M.; Staebler, R. M.; Moussa, S. G.;  
 388 Darlington, A.; Wolde, M.; Thompson, D.; Chen, J.; Griffin, D.; Eckert, E.; Ditto, J. C.; He,  
 389 M.; Gentner, D. R. Reconciling the Total Carbon Budget for Boreal Forest Wildfire  
 390 Emissions Using Airborne Observations. *Atmos Chem Phys* **2022**, 22 (18), 12493–12523.  
 391 <https://doi.org/10.5194/acp-22-12493-2022>.

- 392 (34) Ye, R. X.; Di Lorenzo, R. A.; Clouthier, J. T.; Young, C. J.; VandenBoer, T. C. A Rapid  
393 Derivatization for Quantitation of Perfluorinated Carboxylic Acids from Aqueous Matrices  
394 by Gas Chromatography-Mass Spectrometry. *Anal Chem* **2023**, *95* (19), 7648–7655.  
395 <https://doi.org/10.1021/acs.analchem.3c00593>.
- 396 (35) Joudan, S.; Gauthier, J.; Mabury, S.; Young, C. Aqueous Leaching of Ultra-Short Chain  
397 PFAS from (Fluoro)Polymers: Targeted and Non-Targeted Analysis. *Environ Sci Technol*  
398 *Lett* **2023**, *Submitted*.
- 399 (36) Bertram, T. H.; Kimmel, J. R.; Crisp, T. A.; Ryder, O. S.; Yatavelli, R. L. N.; Thornton, J.  
400 A.; Cubison, M. J.; Gonin, M.; Worsnop, D. R. A Field-Deployable, Chemical Ionization  
401 Time-of-Flight Mass Spectrometer. *Atmos Meas Tech* **2011**, *4* (7), 1471–1479.  
402 <https://doi.org/10.5194/amt-4-1471-2011>.
- 403 (37) Dörich, R.; Eger, P.; Lelieveld, J.; Crowley, J. N. Iodide CIMS and m/z 62: The Detection  
404 of HNO<sub>3</sub> as NO<sub>3</sub>-in the Presence of PAN, Peroxyacetic Acid and Ozone. *Atmos Meas*  
405 *Tech* **2021**, *14* (8), 5319–5332. <https://doi.org/10.5194/amt-14-5319-2021>.
- 406 (38) Zhang, W.; Zhang, H. Secondary Ion Chemistry Mediated by Ozone and Acidic Organic  
407 Molecules in Iodide-Adduct Chemical Ionization Mass Spectrometry. *Anal Chem* **2021**, *93*  
408 (24), 8595–8602. <https://doi.org/10.1021/acs.analchem.1c01486>.
- 409 (39) Lee, B. H.; Lopez-Hilfiker, F. D.; Mohr, C.; Kurtén, T.; Worsnop, D. R.; Thornton, J. A. An  
410 Iodide-Adduct High-Resolution Time-of-Flight Chemical-Ionization Mass Spectrometer:  
411 Application to Atmospheric Inorganic and Organic Compounds. *Environ Sci Technol*  
412 **2014**, *48* (11), 6309–6317. <https://doi.org/10.1021/es500362a>.
- 413 (40) Nah, T.; Ji, Y.; Tanner, D. J.; Guo, H.; Sullivan, A. P.; Ng, N. L.; Weber, R. J.; Huey, L. G.  
414 Real-Time Measurements of Gas-Phase Organic Acids Using SF<sub>6</sub>- Chemical Ionization  
415 Mass Spectrometry. *Atmos Meas Tech* **2018**, *11* (9), 5087–5104.  
416 <https://doi.org/10.5194/amt-11-5087-2018>.

- 417 (41) Zehavi, D.; Seiber, J. N. An Analytical Method for Trifluoroacetic Acid in Water and Air  
418 Samples Using Headspace Gas Chromatographic Determination of the Methyl Ester.  
419 *Anal Chem* **1996**, 68 (19), 3450–3459. <https://doi.org/10.1021/ac960128s>.
- 420 (42) Hu, X.; Wu, J.; Zhai, Z. H.; Zhang, B. Y.; Zhang, J. B. Determination of Gaseous and  
421 Particulate Trifluoroacetic Acid in Atmosphere Environmental Samples by Gas  
422 Chromatography-Mass Spectrometry. *Fenxi Huaxue/ Chinese Journal of Analytical*  
423 *Chemistry* **2013**, 41 (8), 1140–1145. [https://doi.org/10.1016/S1872-2040\(13\)60676-3](https://doi.org/10.1016/S1872-2040(13)60676-3).
- 424 (43) Zhang, B.; Zhai, Z.; Zhang, J. Distribution of Trifluoroacetic Acid in Gas and Particulate  
425 Phases in Beijing from 2013 to 2016. *Science of the Total Environment* **2018**, 634, 471–  
426 477. <https://doi.org/10.1016/j.scitotenv.2018.03.384>.
- 427 (44) Tian, Y.; Yao, Y.; Chang, S.; Zhao, Z.; Zhao, Y.; Yuan, X.; Wu, F.; Sun, H. Occurrence  
428 and Phase Distribution of Neutral and Ionizable Per- and Polyfluoroalkyl Substances  
429 (PFASs) in the Atmosphere and Plant Leaves around Landfills: A Case Study in Tianjin,  
430 China. *Environ Sci Technol* **2018**, 52 (3), 1301–1310.  
431 <https://doi.org/10.1021/acs.est.7b05385>.
- 432 (45) Arp, H. P. H.; Goss, K. U. Gas/Particle Partitioning Behavior of Perfluorocarboxylic Acids  
433 with Terrestrial Aerosols. *Environ Sci Technol* **2009**, 43 (22), 8542–8547.  
434 <https://doi.org/10.1021/es901864s>.
- 435 (46) Tao, Y.; VandenBoer, T. C.; Ye, R. X.; Young, C. J. Exploring Controls on  
436 Perfluorocarboxylic Acid (PFCA) Gas-Particle Partitioning Using a Model with  
437 Observational Constraints. *Environ Sci Process Impacts* **2022**, 25 (2), 264–276.  
438 <https://doi.org/10.1039/d2em00261b>.
- 439 (47) Barton, C. A.; Kaiser, M. A.; Russell, M. H. Partitioning and Removal of  
440 Perfluorooctanoate during Rain Events: The Importance of Physical-Chemical Properties.  
441 *Journal of Environmental Monitoring* **2007**, 9 (8), 839. <https://doi.org/10.1039/b703510a>.

- 442 (48) Geddes, J. A.; Murphy, J. G.; Wang, D. K. Long Term Changes in Nitrogen Oxides and  
443 Volatile Organic Compounds in Toronto and the Challenges Facing Local Ozone Control.  
444 *Atmos Environ* **2009**, *43* (21), 3407–3415.  
445 <https://doi.org/10.1016/j.atmosenv.2009.03.053>.
- 446 (49) Pugliese, S. C.; Murphy, J. G.; Geddes, J. A.; Wang, J. M. The Impacts of Precursor  
447 Reduction and Meteorology on Ground-Level Ozone in the Greater Toronto Area. *Atmos*  
448 *Chem Phys* **2014**, *14*, 8197–8207. <https://doi.org/10.5194/acp-14-8197-2014>.
- 449 (50) Cai, C.; Avise, J.; Kaduwela, A.; DaMassa, J.; Warneke, C.; Gilman, J. B.; Kuster, W.; de  
450 Gouw, J.; Volkamer, R.; Stevens, P.; Lefer, B.; Holloway, J. S.; Pollack, I. B.; Ryerson, T.;  
451 Atlas, E.; Blake, D.; Rappenglueck, B.; Brown, S. S.; Dube, W. P. Simulating the Weekly  
452 Cycle of NO<sub>x</sub>-VOC-HO<sub>x</sub>-O<sub>3</sub> Photochemical System in the South Coast of California  
453 During CalNex-2010 Campaign. *Journal of Geophysical Research: Atmospheres* **2019**,  
454 *124* (6), 3532–3555. <https://doi.org/10.1029/2018JD029859>.
- 455 (51) Young, C. J.; Mabury, S. A. Atmospheric Perfluorinated Acid Precursors: Chemistry,  
456 Occurrence and Impacts. *Rev Environ Contam Toxicol* **2010**, *208*, 1–110.  
457 [https://doi.org/10.1007/978-1-4419-6880-7\\_1](https://doi.org/10.1007/978-1-4419-6880-7_1).
- 458 (52) Yarwood, G.; Kemball-Cook, S.; Keinath, M.; Waterland, R. L.; Korzeniowski, S. H.; Buck,  
459 R. C.; Russell, M. H.; Washburn, S. T. High-Resolution Atmospheric Modeling of  
460 Fluorotelomer Alcohols and Perfluorocarboxylic Acids in the North American  
461 Troposphere. *Environ Sci Technol* **2007**, *41*, 5756–5762.
- 462 (53) Kotamarthi, V. R.; Rodriguez, J. M.; Ko, M. K. W.; Tromp, T. K.; Sze, N. D.; Prather, M. J.  
463 Trifluoroacetic Acid from Degradation of HCFCs and HFCs: A Three-Dimensional  
464 Modeling Study. *J Geophys Res* **1998**, *103* (D5), 5747–5758.  
465 <https://doi.org/10.1029/97JD02988>.

466 (54) Kanakidou, M.; Dentener, J.; Crutzen, P. J. A Global Three-Dimensional Study of the  
 467 Fate of HCFCs and HFC-134a in the Troposphere. *J Geophys Res* **1995**, *100* (D9),  
 468 18781–18801. <https://doi.org/10.1029/95JD01919>.

469 (55) Holland, R.; Khan, M. A. H.; Driscoll, I.; Chhantyal-Pun, R.; Derwent, R. G.; Taatjes, C.  
 470 A.; Orr-Ewing, A. J.; Percival, C. J.; Shallcross, D. E. Investigation of the Production of  
 471 Trifluoroacetic Acid from Two Halocarbons, HFC-134a and HFO-1234yf and Its Fates  
 472 Using a Global Three-Dimensional Chemical Transport Model. *ACS Earth Space Chem*  
 473 **2021**, *5* (4), 849–857. <https://doi.org/10.1021/acsearthspacechem.0c00355>.

474 (56) Neuman, J. A.; Huey, L. G.; Ryerson, T. B.; Fahey, D. W. Study of Inlet Materials for  
 475 Sampling Atmospheric Nitric Acid. *Environ Sci Technol* **1999**, *33* (7), 1133–1136.  
 476 <https://doi.org/10.1021/es980767f>.

477 (57) Halfacre, J. W.; Stewart, J.; Herndon, S. C.; Roscioli, J. R.; Dyroff, C.; Yacovitch, T. I.;  
 478 Flynn, M.; Andrews, S. J.; Brown, S. S.; Veres, P. R.; Edwards, P. M. Using Tunable  
 479 Infrared Laser Direct Absorption Spectroscopy for Ambient Hydrogen Chloride Detection:  
 480 HCl-TILDAS. *Atmos Meas Tech* **2023**, *16* (5), 1407–1429. [https://doi.org/10.5194/amt-16-](https://doi.org/10.5194/amt-16-1407-2023)  
 481 [1407-2023](https://doi.org/10.5194/amt-16-1407-2023).  
 482